Unviersty of Anbar

Anbar Journal Of Engineering Science©

journal homepage: http:// http://www.uoanbar.edu.iq/Evaluate/

Assessment the Shear Behavior of Sustainable Thick Hollow Core Slab Using Experimental and Nonlinear Finite Element Modelling

Yousif Nassif Sabr [a*], Dr. Husain Khalaf Jarallah [b], Dr. Hassan Issa AbdulKareem [c]

[a] *Civil Engineering Department, Mustansiriyah University, Baghdad, Iraq (M.Sc. Student)*
[b] *Civil Engineering Department, Mustansiriyah University, Baghdad, Iraq (Assist Prof.)*
[c] *Civil Engineering Department, Mustansiriyah University, Baghdad, Iraq (Assist Prof.)*

PAPER INFO

Paper history:
Received … … …
Received in revised form … … …
Accepted … … …

Keywords:
Hollow core slab, Nonlinear Finite element, Lightweight concrete, Improving shear strength and Crushed clay brick.

ABSTRACT

This investigation provides experimental results and nonlinear analysis by using finite element model of thick hollow core slab made from recycled lightweight material. Four hollow core slabs specimens were cast and tested in this investigation with dimensions (1200mm length, 450mm width and 250mm thickness). The crushed clay brick was used as a coarse aggregate instead of gravel. The iron powder waste and silica fume were used in order to increase the compressive strength of concrete. The techniques reduction hollow length and use shear reinforcement were used to improve shear strength and avoid shear failure. The specimens were tested by applying two-line load up to failure. The experimental results were showed these techniques were resisted the shear failure significantly and works to change failure mode from shear to flexural failure. Finite element computer software program (ANSYS) was used to analysis hollow core slabs specimens and compare the experimental results with the theoretical results. Good agreement have been obtained between experimental and numerical results.

1. Introduction

Hollow core slab (HCS) is a precast prestress or non-prestress concrete slab. This slab is contained voids extend throughout the length of the slab to decrease weight and cost. This slab is utilized to disguise electrical or mechanical runs. Likewise, HCS has application as spandrel members, wall panels, and bridge deck units. Span length of HCS reaches up to (18m) without columns or any supporting members. HCS system can be utilized for an extensive variety of utilization requiring floor or roof systems. HCS system provides extreme structural efficiency, also at the same time requiring low material consumption [1].

Al-Azzawi and Abed (2016) [2] studied the HCS system through experimental and theoretical investigation. HCS specimens were different in hollow diameter, different in shear span to depth ratio (a/d) and solid slab for comparison with HCS specimens. The experimental results showed decrease in ultimate load in solid slab with increase (a/d). Ultimate load in HCS specimens decrease about (5.49%, 15.7% and 20.6%) with increase the hollow diameter from 75mm to 100mm and 150mm. Increase (a/d) in HCS specimens from 2 to 2.5 and 3 were showed decreasing in ultimate load about (31% and 45%) respectively. The FEM was used to analysis the experimental specimens, where showed good agreement with the experimental results.

Dudnik et al. (2017) [3] investigate add steel fiber in concrete to resist the shear failure at HCS specimens. The experimental work was included cast twenty prestress HCS specimens with and without steel fiber. The main variables were the volume of

* Corresponding author. Tel.: 07903558003

yousifnasef@gmail.com

steel fiber (0.38%, 0.5% and 0.76%), the thickness of HCS specimens (300mm and 410mm) and the shear span to depth ratio (3 and 3.5). The test was done under applied one line load near to the support with different shear span to depth ratio. The specimens with steel fiber increase in shear strength of about 55% to 90% compare with the HCS specimens without steel fiber. Generally, add steel fiber lead to increase ductility.

El-Arab (2017) [4] provided a description of the technique to resist the shear cracking in deep HCS specimens under uniform load. Ten HCS specimens were cast with thickness 400mm and 500mm and fill the hollow core with concrete for 1.5m at end of each side. Each thickness was filled voids by concrete from one void to four voices . Steel hook insert in the voids that filed in concrete. The result were showed HCS specimens with thickness 400mm increase in shear capacity by filling the voids from one void to four voids about 68%, 134%, 199% and 256% respectively. The result of the HCS specimens with thickness 500mm showed an increase in web shear capacity by filling the voids from one void to four voids about 55%, 111%, 151% and 197% compared with the HCS specimen without filling the voids.

Lightweight concrete (LWC) has successfully been utilized for long times for structural members and systems in building and bridges. In addition, it is lighter weight, which grants sparing in dead loads and thus decreases the costs of both superstructure and foundation. It is impervious to fire and gives preferable heat and sound protection than concrete of normal density [5] [6]. LWC is considered as having a density not exceeding 1920 kg/m^3, while normal density concrete is considered to have a usual density ranging between 2240 kg/m^3 and 2480 kg/m^3, and the minimum compressive strength at 28 days is 17 MPa [7]. LWC with cylinder compressive strength (f 'c) greater than 41 MPa was characterized as high strength concrete (HSC) [7].

2. Research Significance

The structural behavior of the sustainable high strength LWC nonprestress thick HCS made from recycled material (crushed clay brick (CCB) and iron powder waste (IPW)) are study in this research paper.

3. HCS Specimens and Test Parameters

The description of tested HCS are given in Table 1 below. Each slab has three hollow cores. The experimental program includes casting and testing four HCS specimens. The HCS specimens were selected to be thick (the thickness to clear length ratio h/l_n <1/5 where h is thickness of slab and l_n is clear span [8]). The details of HCS specimens are shown in Figures 1, 2, 3 and 4. The HCS specimens were designed according to ACI-318M-14 [9]. The lightweight concrete is used in this research by using crushed clay brick (CCB) as a coarse aggregate. The silica fume and iron powder waste were used to reach high strength lightweight concrete. The details of concrete mix and mechanical properties shown in the Table 2. The density of tested mix was 1910kg/m^3 accordingly the concrete will be specified as LWC [7].The test of steel reinforcement was done according to ASTM A615 and ASTM A496 [10, 11]. The properties of steel reinforcement shown in Table 3.

Table 1. HCS Dimensions

HCS ID*	Length (mm)	Width (mm)	Thickness (mm)	Parameter
HCS-250-A	1200	450	250	Contain three hollow core.
HCS-250-B	1200	450	250	Reduction one hollow length.
HCS-250-C	1200	450	250	Reduction two hollow length.
HCS-250-D	1200	450	250	Use shear reinforcement.

*A=HCS specimens contain three hollows along entire length of HCS (1200mm) and without shear reinforcement.

B= HCS specimens contain two hollows along entire length of HCS (1200mm) and one hollow along the length 600mm in the mid-span and without shear reinforcement.

C=HCS specimens contain one hollow along entire length of HCS (1200mm) and two hollows along the length 600mm in the mid-span and without shear reinforcement.

D=HCS specimens contain three hollows along entire length of HCS (1200mm) and with shear reinforcement.

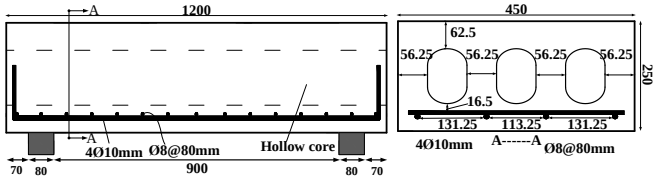

Section and side view

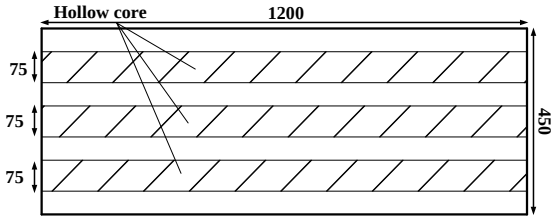

Top view

Figure 1. HCS Specimen (HCS-250-A) (All Dimensions in mm)

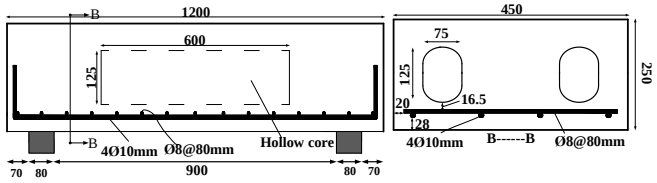

Section and side view

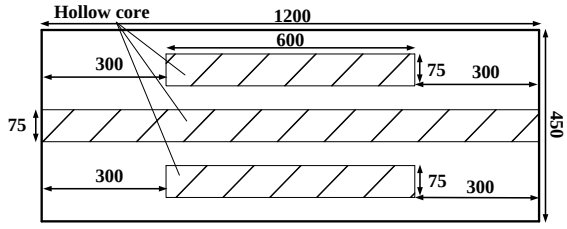

Top view

Figure 2. HCS Specimen (HCS-250-B) (All Dimensions in mm)

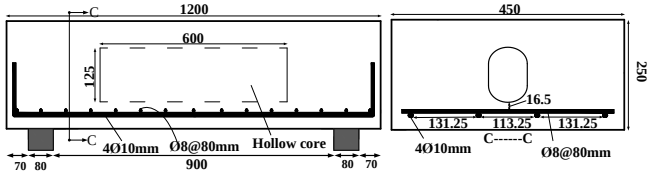

Section and side view

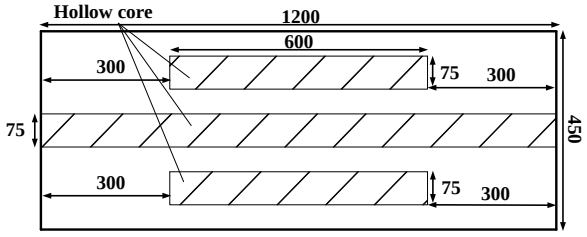

Top view

Figure 3. HCS Specimen (HCS-250-C) (All Dimensions in mm)

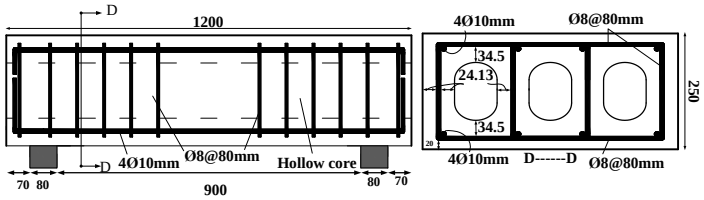

Section and side view

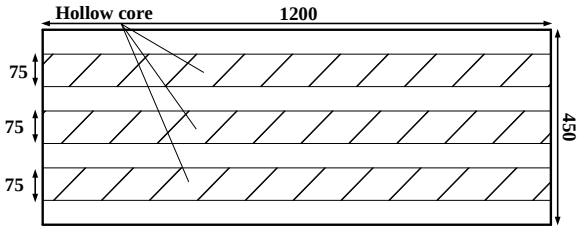

Top view

Figure 4. HCS Specimen (HCS-250-D) (All Dimensions in mm)

Table 2. Details of Concrete Mix

Parameter	Content
Cement (kg/m^3)	485
Sand (kg/m^3)	500
CCB* (kg/m^3)	712
SF* (kg/m^3)	48.5
IPW* (kg/m^3)	4.85
Superplasticizer L/m^3	4.85
W/C	0.31
Mechanical Properties of Concrete	
Cylinder Compressive strength	42.3 MPa
Modulus of Elasticity (E_c)	24147 MPa
Poisson's ratio (ν)	0.23

*CCB= Crushed Clay Brick, SF= Silica Fume, IPW= Iron Powder Waste

Table 3. Details of Test Steel Reinforcement*

Bar Nominal Diameter (mm)	8	10
Bar Measure Diameter (mm)	7.83	10.05
Bar Type	Deformed	Deformed
Yield Strength (fy) (MPa)	582	524
Ultimate Strength (fu) (MPa)	696	650
Elongation (%)	12.5	13

*Each value is an average of three specimens (each 50 cm length)

The HCS specimens were tested under two line load as shown in Figures 5 and 6. The dial gauge was installed in the mid span to measure the maximum deflection.

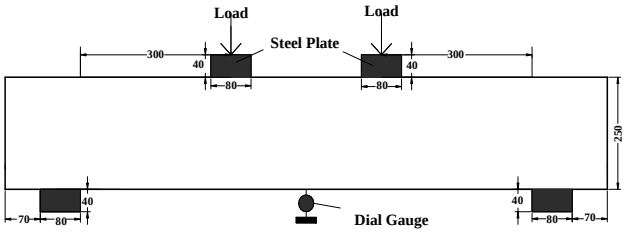

Figure 5. Location of the Dial Gauge

Figure 6. The HCS Specimen in the Machine Test

4. FEM Modeling of HCS

A nonlinear finite element analysis has been carried out to analyze all experimentally tested specimens of HCS. The analysis was performed by ANSYS software program (Version 15) [12]. The elements used for modeling the components of the HCS specimens were showed in Table 4. The real constants are needed to represent the geometrical properties of the used elements such as cross-sectional area for steel reinforcement. The material properties are needed to represent the behavior and characteristics of the constitutive materials depending on mechanical tests such as density, modulus of elasticity and Poisson`s ratio as shown in the Table 5. In ANSYS software program the analysis was done by taking the quarter of the HCS specimen by symmetrical boundary conditions and loading as shown in the Figure 7.

Table 4. Characteristics of the Selected Elements

Panel Component	Element Type	Element Characteristics
Concrete	Solid65	8-node brick linear element
Reinforced Bars	Link180	2-node linear 3D truss element
Steel plate	Solid45	8- nodes and the isotropic material properties with elastic linear behavior

Table 5. Material Properties and Parameters for Non-Linear Solution

Element Type	Material Properties			Details
Solid65	Linear Isotropic	Modulus of elasticity (MPa)		24147
		Poisson's ratio		0.23
	Concrete Properties	Open Shear Transfer Coefficient		0.7*
		Closed Shear Transfer Coefficient		0.95*
		Uniaxial Cracking Stress		3.1
		Uniaxial Crushing Stress		42.3
		Density (kg/m3)		1910
Link180	Ø10mm	Linear Isotropic	Modulus of elasticity (MPa)	200000*
			Poisson's ratio	0.3*
		Bilinear Isotropic	Yield stress (MPa)	524
			Hardening Tangent Modulus (MPa)	2000*
	Ø8mm	Linear Isotropic	Modulus of elasticity (MPa)	200000*
			Poisson's ratio	0.3*
		Bilinear Isotropic	Yield stress (MPa)	582
			Hardening Tangent Modulus (MPa)	2000*
Solid45	Linear Isotropic	Modulus of elasticity (MPa)		200000*
		Poisson's ratio		0.3*

*This value is assume to give convergence nonlinear finite element analysis and provide good results as compare with experimental results.

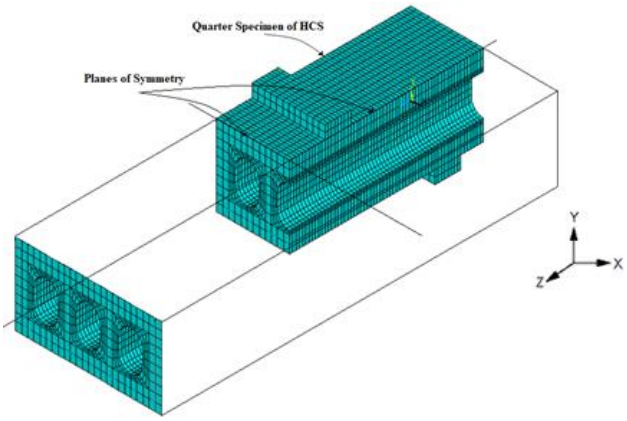

Figure 7. Quarter Specimens of HCS

A significant stage in the FEM analyses modeling was choice the mesh. In this work, the model volume of HCS specimens closed with different size of mesh (25mm thick, 18.75mm width, and 10mm length) for each element of concrete. The meshing of HCS specimens with circular and noncircular core shape is difficult because of the need to the fine mesh for analyses. The way used in this work to prepare uniform mesh in the section area by forming four areas greater than the dimensions of the circular and noncircular void, then drawing the void inside the four areas and subtracting the areas from the void. Divided the lines of cross section and extrude the area of the cross-section with length 600mm to reach the model volume, and then meshing this volume using the solid64 element as shown in the Figure 8. The boundary conditions were needed for quarter HCS specimen at the symmetry plane in X-direction and Z-direction, where restrict the movement in the perpendicular direction on the symmetry plane. The support has restricted the movement in X and Y-direction at the nodes a long line of center steel plate. The load was applied also at the nodes a long line of center steel plate. The number of element shown in the Table 6.

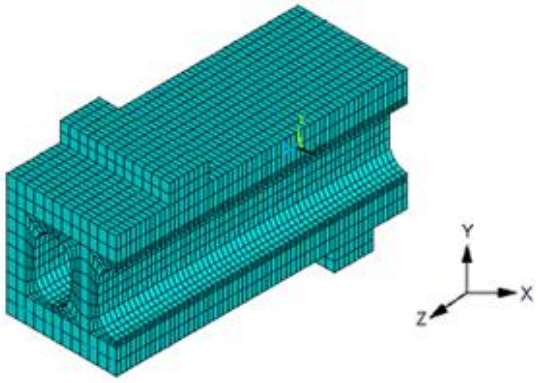

Figure 8. Mesh of HCS Specimen

Table 6. Number of Element

HCS ID	Number of Elements			Total
	Solid65	Link180	Solid45	
HCS-250-A	10440	214	384	11038
HCS-250-B	9900	214	384	10498
HCS-250-C	9360	214	384	9958
HCS-250-D	10440	462	384	11286

The longitudinal and transverse steel reinforcement was modeled by link180 element. The details of the steel reinforcement between the concrete element for HCS specimens HCS-250-A, HCS-250-B and HCS-250-C shown in the Figure 9 and for HCS-250-D shown in the Figure 10.

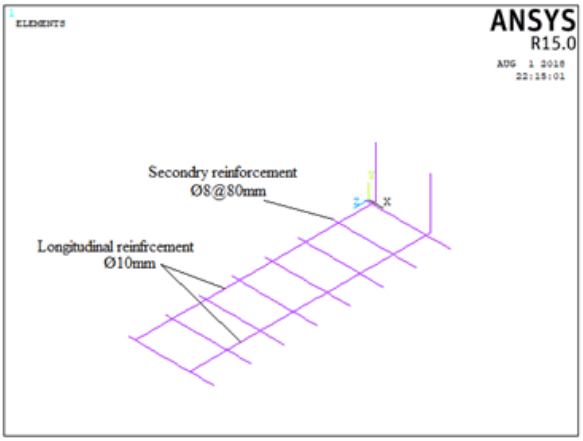

Figure 9. Steel Reinforcement for Quarter HCS Specimens for HCS Specimens HCS-250-A, HCS-250-B and HCS-250-C

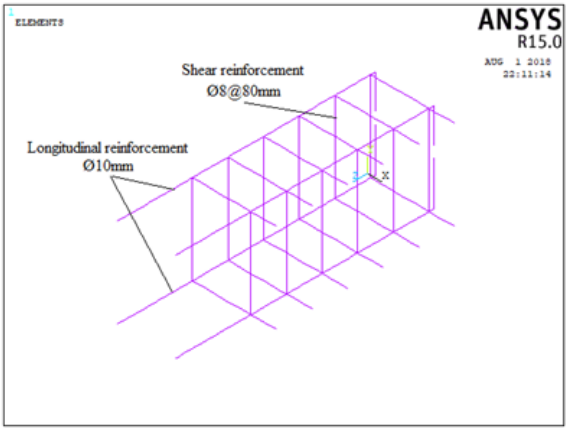

Figure 10. Steel Reinforcement for Quarter HCS-250-D

5. Failure Criteria for Concrete

The failure patterns were occurred in concrete are cracking failure and crushing failure. The tensile and compressive strengths are desired to characterize the failure at concrete [13]. A three-dimensional failure surface for concrete shown in the Figure 11. Three failure surfaces are shown on the (σxp-σyp) plane. The patterns of failure are depending on σZP (stress in σZP direction). Such as, if σxp and σyp, both are negative (compressive) and σZP is positive (tensile), cracking would prophesy in a trend perpendicular to σZP. However, if σZP is zero or negative, the material is assume crush. For concrete element, when the principal tensile stress in any direction outside the surface of failure the cracking occur. The elastic modulus of the concrete element is set to zero in the direction parallel to the principal tensile stress. While the crush occur when all stresses are compressive and located outside the failure surface. Thereafter, the elastic modulus is set to zero in all directions [12].

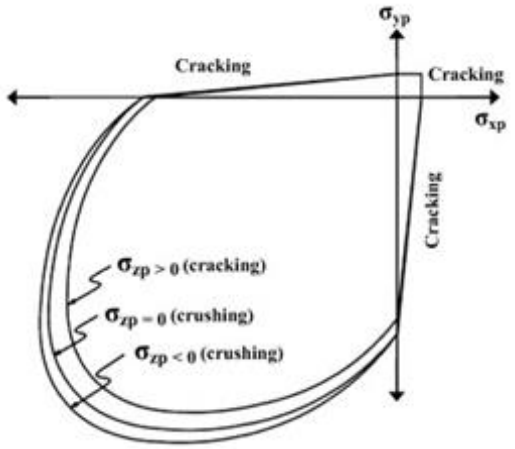

Figure 11. 3-D Failure Surface for Concrete [10]

6. Results and Discussion

6.1. Experimental Results

6.1.1. Ultimate and First Crack Load

The load was applied with steps 5kN with the record the deflection for each load step. At early the HCS specimens free of apparent cracks. With increasing the load, the first crack can be seen at the mid-span in the tension zone. Increase the load more several cracks were become faster and spacious. The load continues to the extent of specimen failure. The experimental results of HCS specimens shown in Table 7. The crack pattern of specimens shown in Figure 12. The weight of HCS specimens with ratio of increase due to increase the hollow length shown in Table 8.

Table 7. First and Ultimate Crack Load Results and Weight of HCS Specimens

HCS ID	P_u(kN)	P_u(%)	P_{cr}(kN)	P_{cr}(%)
HCS-250-A*	92.5	-	16.1	-
HCS-250-B	137.5	+48.65	19.2	+19.25
HCS-250-C	178	+92.43	23.6	+46.58
HCS-250-D	198	+114	25.8	+60.25

*Reference HCS specimen

Table 8. Weight of HCS Specimens

HCS ID	Unit Weight (Kg)	Weight (%)
HCS-250-A*	201.7	-
HCS-250-B	211	+4.61
HCS-250-C	220.42	+9.28
HCS-250-D	201.7	-

*Reference HCS specimen

From the Results shown in Table 7, the ultimate load and first crack load increase with reduction one and two hollow length and with use shear reinforcement. This is due to increase in the cross-section area at a region near to the support by reduction hollow length from each side of the span. As well as, add shear reinforcement increase the stiffness of the specimen to resist the shear failure. This increase in the ultimate load and first crack load accompanied by a slight increase in weight as shown in Table 8. These techniques are resist the shear failure and work to convert the load to the mid-span thus change the failure mode.

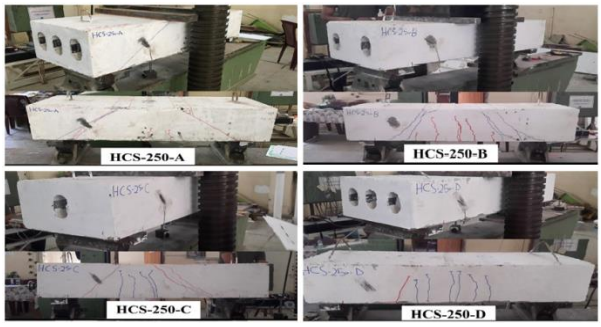

Figure 12. Crack Pattern for HCS Specimens

6.1.2. Load-Deflection Relationship

The experimental results of deflection shown in the Table 9 and the load-deflection curve for HCS specimens shown in Figure 13. The reduction in the

length one and two hollow lengths from each side of HCS specimens and add shear reinforcement lead to increase the maximum deflection in the mid-span. The reduction hollow length and add shear reinforcement gives more resisting to the shear failure, and change the mode of failure to the flexural-shear and flexural failure. The ductile behavior was observe for specimen HCS-250-D.

Table 9. Maximum Deflection for HCS Specimens

HCS ID	Δu (mm)	Δu (%)
HCS-250-A*	3.5	-
HCS-250-B	3.8	+8.57
HCS-250-C	4.1	+17.14
HCS-250-D	4.3	+22.86

*Reference HCS specimen

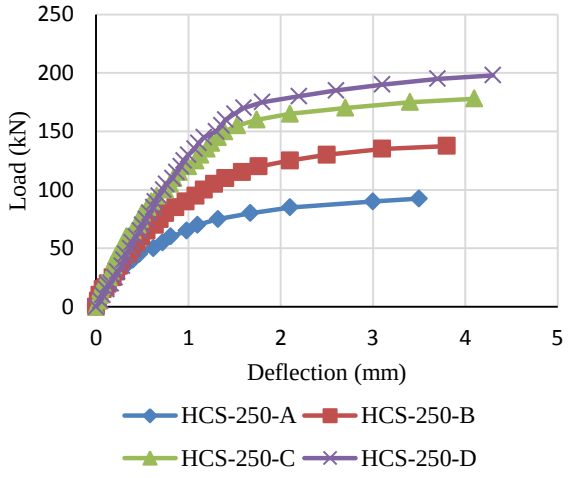

Figure 13. Load-Deflection Curve for HCS Specimens

6.2. Comparison of Numerical and Experimental Results

6.2.1. Load-Deflection Curve

The numerical and experimental results of the ultimate load and the maximum deflection shown in Table 10 and Table 11. The numerical and experimental load-deflection responses for the tested specimens were showed in Figures 14 through 17. The results of load-deflection, maximum deflection and ultimate load of specimens from the finite element analysis referred a good agreement with the results from the experimental test of specimens. The difference between experimental work and numerical analysis is about (3%) in ultimate load and about (88%) in maximum deflection. These ratios are considered reasonable and accepted. This different between the numerical and experimental results due to the ideal condition of concrete homogeneity assumed in the numerical solution which results in greater stiffness than experimental results.

Table 10. Numerical and Experimental Results for Ultimate Load

HCS ID	$P_{u\ Exp.}$*	$P_{u\ Num.}$**	$P_{u\ Num.}/P_{u\ Exp.}$
HCS-250-A	92.5	97.65	1.056
HCS-250-B	137.5	139.4	1.014
HCS-250-C	178	184.5	1.037
HCS-250-D	198	202.5	1.023
	Average		1.0325

*Ultimate load from experimental results
**Ultimate load from numerical results

Table 11. Numerical and Experimental Results for Maximum Deflection

HCS ID	$\Delta_{u\ Exp.}$	$\Delta_{u\ Num.}$	$\Delta_{u\ Num.}/\Delta_{u\ Exp.}$
HCS-250-A	3.5	3.2	0.91
HCS-250-B	3.8	3.49	0.92
HCS-250-C	4.1	3.57	0.87
HCS-250-D	4.3	3.66	0.85
	Average		0.8875

*Maximum deflection from experimental results
**Maximum deflection from numerical results

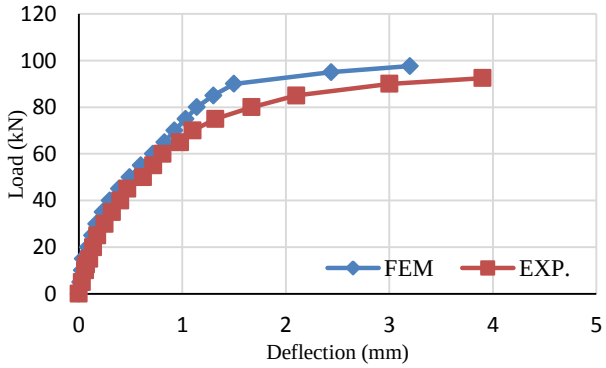

Figure 14. Load-Deflection Relationship for HCS-250-A

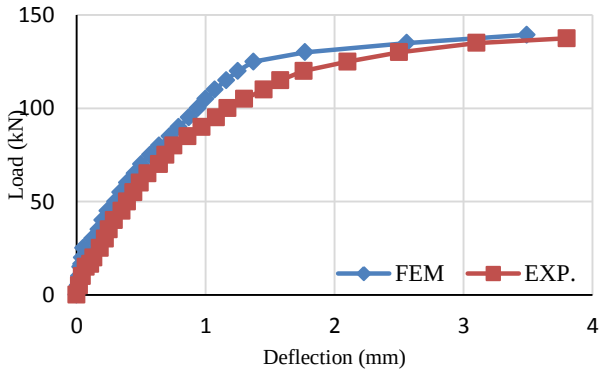

Figure 15. Load-Deflection Relationship for HCS-250-B

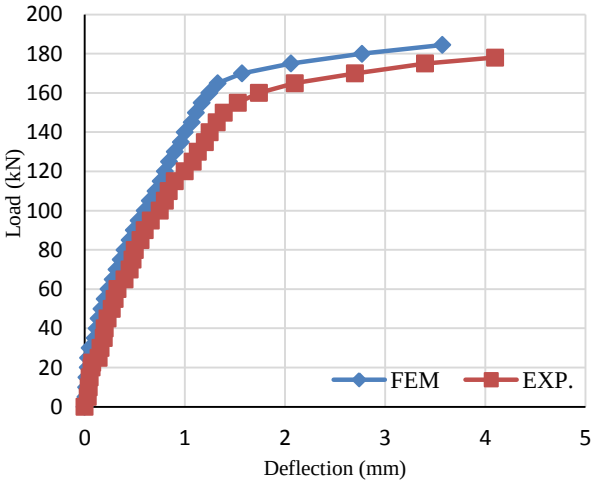

Figure 16. Load-Deflection Relationship for HCS-250-C

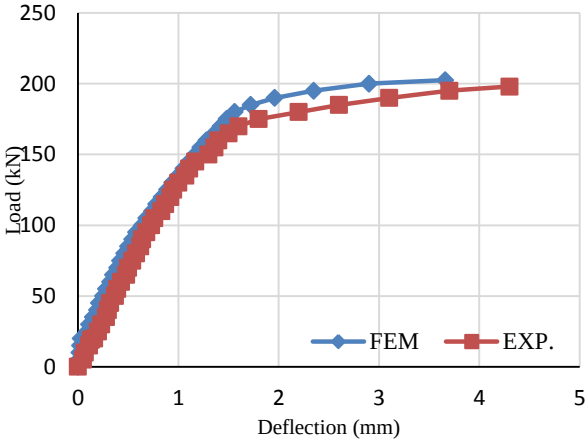

Figure 17. Load-Deflection Relationship for HCS-250-D

6.2.2. Crack Pattern

The crack pattern for HCS specimens from the numerical and experimental work shown in the Figure 18 given a good agreement between the numerical and experimental work.

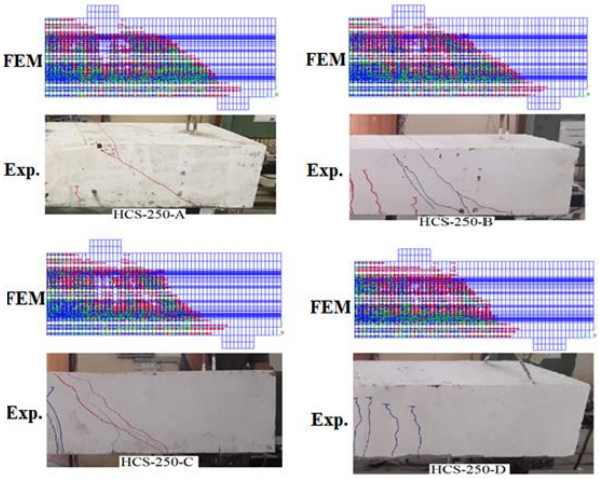

Figure 18. Comparison of Crack Pattern of HCS Specimens between Finite Element Analysis and Experimental Work

7. Conclusions

Depending on the results from experimental and numerical work, the following main conclusions are presented:

1-The techniques were used to resist shear failure showed an increase in the ultimate load, first crack load and in the maximum deflection up to 114%, 60.25% and 22.86% respectively.

2-Improve the shear strength of HCS specimens by reduction in one and two hollow lengths and use shear reinforcement change the mode failure from the shear failure to flexural failure. The select the critical hollow length is required more studies by using different hollow core length.

3- The results of finite element analysis showed the ultimate load and maximum deflection values were closed form the results of excremental investigation. The good agreement between the finite element analysis and the experimental investigation about (97%) for the ultimate load and about (88%) for the maximum deflection.

4-The crack pattern at the ultimate load in the finite element analysis was comparable with mode failure in the experimental test.

8. References

[1] Stephen, C., "Hollow Core Manufacture and Factory Design", the Indian Concrete Journal 2013.pp 20-25.

[2] Al-Azzawi, A. A. and Abed, S. A. "Numerical Analysis of Reinforced Concrete Hollow- Core Slabs", ARPN Journal of Engineering and Applied Science. 11(15), 2016.

[3] Dudnik, V. S., Milliman, L. R. and Parra-Montesinos, G. J., "Shear Behavior of Prestressed Steel-Fiber-Reinforced Concrete Hollow-Core Slabs", PCI Journal, July–August 2017.

[4] El-Arab, I. M. E., "Web Shear Strengthening Technique of Deep Precast Prestressed Hollow Core Slabs under Truck Loads", Journal of Building Construction and Planning Research, 5, 129-145, 2017.

[5] Slate, F. O., Nilson, A. H. and Martinez, S., "Mechanical Properties of High Strength lightweight concrete", ACI Journal, Proceedings V. 83, No. 4, pp.606-613, July-august 1986.

[6] Mays, G. C. and Barner, R. A., "The Performance of Lightweight Aggregate Concrete Structure in Service", The Structure Engineer, Vol. 69, No 20, 15, pp. 351-360, October 1994.

[7] ACI Committee 213R-03, "Guide for Structure Lightweight-Aggregate Concrete", American Concrete Institute, USA, pp.1-37, 2003.

[8] Szilard, R., "Theories and Application of Plate Analysis", ISBN 0-471-42989-9 ,John Wiley & Sons, Inc. ,New Jersey, U.S.A, pp.6, 2004.

[9] ACI Committee 318, "Building Code Requirements for Structural Concrete (ACI 318-M14)", American Concrete Institute, Detroit, USA, 2014.

[10] ASTM A615, "Standard Specification for Deformed and Plain Carbon Structural Steel Bars for Concrete Reinforcement", Annual Book of ASTM Standards, Vol.01, No.02, 2005.

[11] ASTM A496, "Standard Specification for Steel Wire, Deformed, for Concrete Reinforcement", Annual Book of ASTM Standards, 1997.

[12] ANSYS 15.0 Manual Set, ANSYS Inc., Canonsburg, PA, 2013.

[13] Willam, K. J. and Warnke, E. P., "Constitutive Model for Triaxial Behavior of Concrete", Seminer on Concrete Structures Subjected to Triaxial Stresses, International Association of Bridge and Structural Engineering Conference, Bergamo, Italy, p.174, 1974.